

First-principles generalized gradient approximation (GGA)+ U^d+U^p studies of electronic structures and optical properties in cubic HfO₂

Jinping Li,^{1,2, a)} Songhe Meng,¹ Lingling Li,¹ Hantao Lu,² and Takami Tohyama²

¹⁾*Center for Composite Materials, Harbin Institute of Technology, Harbin 150080, China*

²⁾*Yukawa Institute for Theoretical Physics, Kyoto University, Kyoto, 606-8502, Japan*

(Dated: 4 April 2024)

The electronic structures and optical properties of cubic HfO₂ are calculated by generalized gradient approximation (GGA)+ U approach. Without on-site Coulomb interactions, the band gap of cubic HfO₂ is 2.92 eV, much lower than the experimental value (5.7 eV). Introducing the Coulomb interactions of 5d orbitals on Hf atom (U^d) and of 2p orbitals on O atom (U^p), we can reproduce the experimental value of the band gap. The calculated dielectric function of cubic HfO₂ by the GGA+ U^d+U^p approach predicts the presence of a shoulder structure below the main peak of the absorption spectrum. These indicate that the GGA+ U^d+U^p approach is a convenient and powerful method to calculate and predict the electronic structures and optical properties of wide-gap optical materials.

PACS numbers: 71.20.Ps, 71.15.Mb, 78.40.Ha

Keywords: cubic HfO₂; first-principles; GGA+ U ; electronic structure; optical properties

^{a)}Electronic mail: lijinpings@hit.edu.cn; jinpings@yukawa.kyoto-u.ac.jp

I. INTRODUCTION

HfO₂ has been widely studied both experimentally and theoretically because of its excellent dielectric properties, wide band gap, high melting point, *etc.*^{1,2}. Moreover, HfO₂ has been proved to be one of the most promising high-dielectric-constant materials, due to its high formation heat and nice thermodynamic stability when it contacts indirectly with Si³. It has also been used in optical⁴ and protective coatings⁵. At atmospheric pressure, HfO₂ exists in three polymorphs when temperature changes⁶: monoclinic structure (P21/c, C2h 5) at low temperatures, tetragonal (P42/nmc, D4h 15) at temperature higher than 2000 K, and finally, with increasing temperature over 2870 K, the cubic fluorite (Fm3m, Oh 5) becomes stable. However, by rapid quenching or stabilizer addition, the cubic structure can be stabilized at low temperatures, e.g., see Refs. 7 and 8.

The electronic and structural properties of HfO₂ have been theoretically studied by the first-principles band structure calculation based on the density-functional theory (DFT). For example, the structure, vibration and lattice dielectric properties of HfO₂ have been investigated in the frame of the local density approximation (LDA) and generalized gradient approximation (GGA)⁹. Based on the ABINIT package, the Born effective charge tensors, phonon frequencies and dielectric permittivity tensors in cubic and tetragonal phases are calculated by LDA¹⁰. The full potential linearized augmented plane-wave method based on the WIEN2k code is also employed to study the structural and electronic properties in the cubic phase¹¹. Further, the spin-orbit effect is estimated within the framework of LDA and GGA¹². The resulting band gap is about 3.65 eV, still smaller than the experimental value (5.7 eV)³, indicating that correlation effects in HfO₂ cannot be ignored.

Jiang *et al.*¹³ have studied the band structures of HfO₂ by the GW approximation, where the self-energy of a many-body system is approximated in terms of the screened Coulomb interaction (W) up to first order, and then correlation effects can be addressed to some extent. The resulting band gap value is 5.2 eV. Although the value is much closer to the experimental one, the GW method is highly cost in terms of numerical demands. Another technique to include correlation effects with relatively less computational effort is the so-called LDA+*U* or GGA+*U* approach, in which the correlation effect is incorporated through the on-site Coulomb interaction *U*¹⁴. As an approximation to GW, GGA(LDA)+*U* approach can reproduce experimental data as accurately as the hybrid functional approach but with

much lower computational efforts¹⁵. It can give a qualitative improvement compared with the LDA, not only for excited-state properties such as energy gaps, but also for ground-state properties such as magnetic moments and interatomic exchange parameters¹⁴. Recently, a GGA+ U approach for CeO_2 has been performed, where not only the on-site U for Ce $4f$ electrons, but also for O $2p$ electrons, are included¹⁶. The choice of U is not unambiguous. Though there are attempts to extract it from the first-principles calculations, it is nontrivial to determine its value a priori. Hence, in practice, U is often fitted to reproduce a certain set of experimental data, such as band gaps and structural properties.

In this paper, we use GGA and GGA+ U schemes formulated by Loschen *et al.*¹⁷, to calculate the lattice parameters, band structures, and optical properties of cubic HfO_2 (c- HfO_2). We find that the value of the band gap can be reproduced by introducing the on-site Coulomb interactions of $5d$ orbitals on Hf atom (U^d) and of $2p$ orbitals on O atom (U^p). We also notice that a shoulder structure below the main peak of the imaginary part of the dielectric constant remains even when U^d and U^p are introduced. This implies that the shoulder structure is robust against the change of band structure due to the Coulomb interactions. We thus expect that the shoulder will appear in absorption measurements for pure c- HfO_2 . These findings imply that the GGA+ U^d+U^p approach is a convenient and powerful method to calculate and predict the electronic structures and optical properties of wide-gap optical materials.

II. COMPUTATIONAL METHODOLOGY

Density functional theory calculations are performed with plane-wave ultrasoft pseudopotential, by using GGA with Perdew-Burke-Ernzerhof (PBE) functional and GGA+ U approach as implemented in the CASTEP code (Cambridge Sequential Total Energy Package)¹⁸. The ionic cores are represented by ultrasoft pseudopotentials for Hf and O atoms. For Hf atom, the configuration is $[\text{Xe}]4f^{14}5d^26s^2$, where the $5d^2$ and $6s^2$ electrons are explicitly treated as valence electrons. For O atom, the configuration is $[\text{He}]2s^22p^4$, and valence electrons include $2s^2$ and $2p^4$. The plane-wave cut off energy is 380 eV. And the Brillouin-zone integration is performed over the $24 \times 24 \times 24$ grid sizes using the Monkhorst-Pack method for cubic structure optimization. This set of parameters assure the total energy convergence of 5.0×10^{-6} eV/atom, the maximum force of 0.01 eV/Å, the maximum stress of 0.02 GPa

and the maximum displacement of $5.0 \times 10^{-4} \text{ \AA}$.

In the following sections, we firstly optimize the geometry structure of c-HfO₂ by the GGA method. Using the optimized structure, we next introduce U^d for Hf 5*d* orbitals and U^p for O 2*p* orbitals. Comparing the numerical values of the band gap with the experimental one, we obtain the best values of U^d and U^p . The electronic structures and optical properties of c-HfO₂ are calculated by means of GGA, without U and with U^d+U^p , respectively. Comparison with available experimental data is presented.

III. RESULTS AND DISCUSSION

A. GGA Calculation

The space group of c-HfO₂ is Fm3m and the local symmetry is O5h. Moreover, c-HfO₂ is fully characterized by a single lattice constant a . The GGA calculation of the perfect bulk c-HfO₂ is performed to determine an optimized a in order to check the applicability and accuracy of the ultrasoft pseudopotential. The optimized a is 0.526 nm, in good agreement with other theoretical values^{9–11,19}. The deviation from experimental values (0.508 nm²⁰ and 0.516 nm¹²) is 3.54% at most. Hereafter, we use this optimized value of a .

The band structure along high-symmetry directions of the Brillouin zone and total density of states (DOS) of c-HfO₂ are shown in Fig. 1. The band structure in Fig. 1(a) shows a direct band gap because the top of the valence bands and the bottom of the conduction bands are found at the same X point. The value of the band gap E_g is around 2.92 eV, much smaller than the experimental value 5.7 eV. This is due to the well-known underestimate of conduction-band energies in *ab initio* calculations: the DFT results often undervalue the energy of 5*d* orbitals of Hf atom, lowering the bottom level of conduction bands. As a result, the band gap obtained by GGA is lower than the experimental one.

The total DOS is presented in Fig. 1(b). There are two parts in the valence band, namely, the lower region from -18.9 eV to -15.2 eV and the upper region from -6.6 eV to 0.1 eV . Figure 1(d) shows that the lower valence bands are predominantly composed of O 2*s*, while the upper valence bands consist of O 2*p* accompanied with hybridization with Hf 5*d* as shown in Fig. 1(c). The conduction bands below 10 eV are mostly composed of Hf 5*d* with some amount of O 2*p*. The 6*s* and 5*p* orbitals of Hf atom also contribute to the conduction

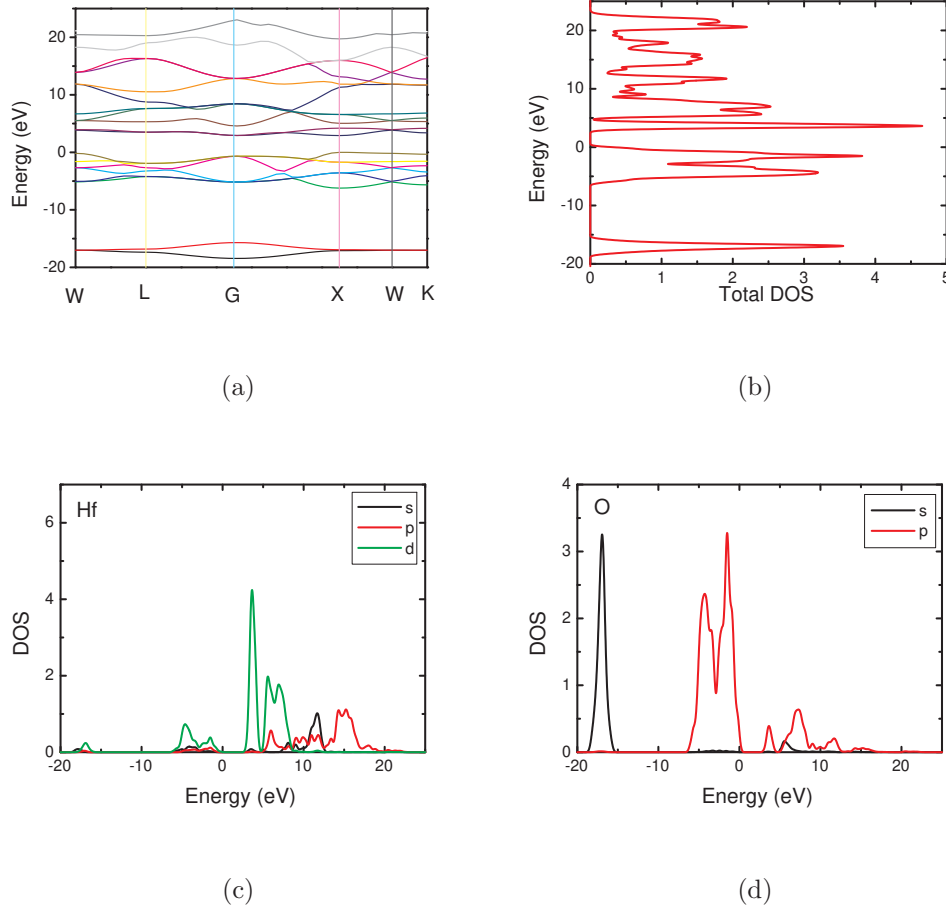


FIG. 1. The band structure and density of states (DOS) of c-HfO₂ obtained by GGA. (a) Band structure; (b) total DOS; (c) partial DOS of Hf atom, and (d) partial DOS of O atom.

bands, though their values are small compared with $5d$ states.

Dielectric function is obtained by taking into account of inter-band transitions. Figure 2 shows the complex dielectric function as a function of photon energy. The real part of the dielectric function ϵ_1 in the low energy increases with photon energy and gets maximum at 3.5 eV. Then it drops sharply with photon energy to negative values and return back to positive later. The imaginary part ϵ_2 shows a maximum at 7.5 eV followed by two shoulder structures below the energy. The two shoulders may be related to DOS in conduction bands at 4 eV and 7 eV as shown in Fig. 1(a). Our results of the dielectric function agree with other calculations for c-HfO₂^{3,21}. However, the magnitude of maximum value of ϵ_2 (~ 10) is larger than an available experimental value (~ 8) of HfO₂²². This disagreement will be resolved if the gap magnitude is reproduced by introducing the on-site Coulomb interactions,

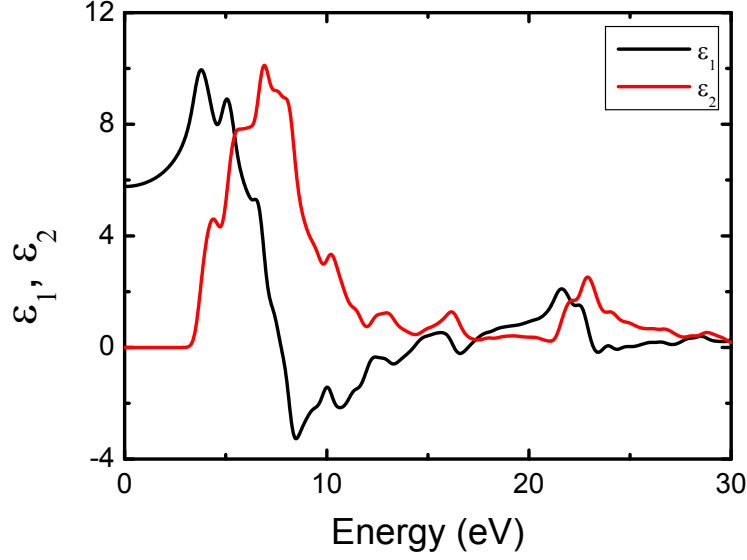


FIG. 2. Real and imaginary parts of dielectric function for c-HfO₂ obtained by GGA.

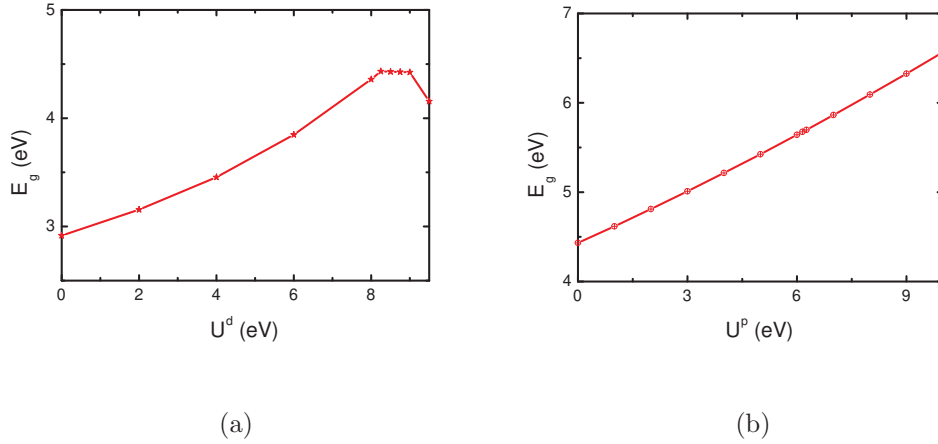


FIG. 3. Calculated band gap E_g as a function of (a) U^d and (b) U^p .

as discussed below.

B. GGA+ U^d+U^p Calculation

Using the optimized lattice parameter, $a = 0.526$ nm, we calculate the band structure and DOS of c-HfO₂ by changing U^d for 5d orbitals of Hf atom. The band gap E_g obtained from the band structure is shown in Fig. 3(a) as a function of U^d . It can be seen that E_g firstly increases, and then drops with increasing U^d , showing a maximum value (4.43 eV)

at $U^d = 8.25$ eV. The maximum value is smaller than the experimental one (5.7 eV). The saturation of E_g with U^d may be related to the approach of $5d$ states toward $6s$ and $5p$ states, though microscopic mechanism is not yet fully understood. Next, we introduce U^p for $2p$ orbital of O atom, while keeping $U^d = 8.25$ eV. The result in Fig. 3(b) shows that E_g monotonically increases with U^p . When $U^d = 8.25$ eV and $U^p = 6.25$ eV, the calculated band gap is 5.697 eV, coinciding with the experiment one.

There could of course exist different combinations of U^d and U^p which can reproduce the band gap. For example, $U^d = 10$ eV, $U^p = 6.35$ eV, the resulting band gap is 5.702 eV, with similar optical properties in the low-energy regime. Based on physical consideration with reference to other numerical results, here, we choose $U^d = 8.25$ eV, $U^p = 6.25$ eV as a typical representative and perform the GGA+ U calculations.

The resulting band structure is shown in Fig. 4(a). The bottom of the conduction bands is moved to the G point. The band dispersions near the bottom shift to higher energy with the increase of U^d and are reconstructed as compared with the dispersions in Fig. 1(a). As a result, the separated DOS at 4 eV and 7 eV in Fig. 1(b) merges to one sharp structure at 6 eV in Fig. 4(b). It is clear from Fig. 4(c) that the reconstruction is caused by the $5d$ state of Hf. The O $2p$ states are also affected by the reconstruction through hybridization effect as seen in Fig. 4(d). We note that the band gap increases with increasing U^p through such strong hybridization effect.

Figure 5 shows the dielectric function. The real part ϵ_1 exhibits a maximum at 6.38 eV, corresponding to band edge reflection peak at 5.0 eV in the reflection spectrum. The calculated static dielectric constant is 3.44, coinciding with the experimental value of monoclinic HfO_2 ^{3,23}. The imaginary part ϵ_2 shows a maximum at 8 eV. The maximum value (~ 7.6) is very close to the experimental value (~ 8)²², in contrast with the GGA case as mentioned before. This improvement comes from the agreement of E_g between the numerical and experimental values. Another interesting observation in ϵ_2 is the presence of a shoulder structure below the peak. It is remarkable that, even though the reconstruction of the band structure occurs near the bottom of the conduction band, the shoulder structure remains as is the case of the GGA calculation. This implies the robustness of the shoulder structure in c- HfO_2 . Therefore, we can expect that such a shoulder structure appears in the absorption spectrum in pure c- HfO_2 samples.

Other optical properties can be computed from the complex dielectric function²⁰. We have

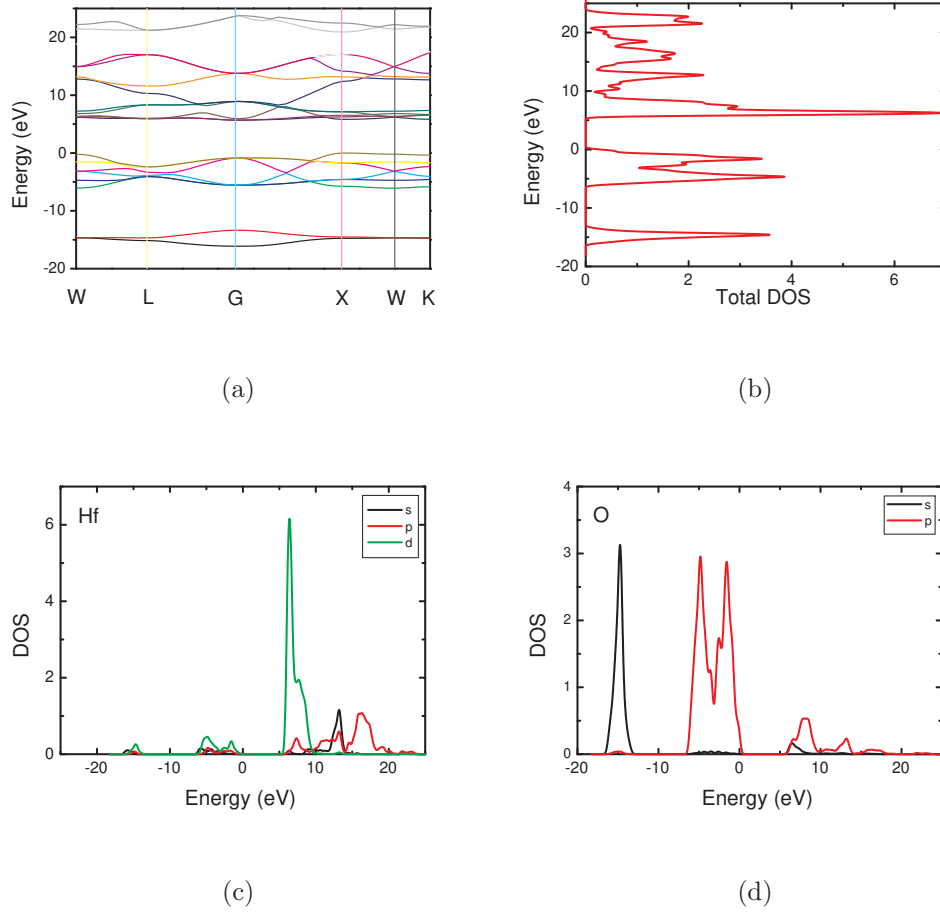


FIG. 4. The band structure and density of states (DOS) of c-HfO₂ obtained by GGA + U^d ($U^d = 8.25$ eV) + U^p ($U^p = 6.25$ eV). (a) Band structure; (b) total DOS; (c) partial DOS of Hf atom, and (d) partial DOS of O atom.

calculated the refractive index of c-HfO₂ by GGA+ U^d+U^p , including refractive coefficient n and extinction coefficient k . The results show that n is 1.85, consistent with the experimental value of monoclinic HfO₂, 1.93³.

IV. CONCLUSIONS

The structure optimization of c-HfO₂ is performed by using first-principles GGA and the resulting cell parameter of optimization structure is 0.526 nm, consistent with the experimental value and other theoretical results. However, the numerical value of band gap is only 2.92 eV, much lower than the experimental ones. The deviation can be resolved by

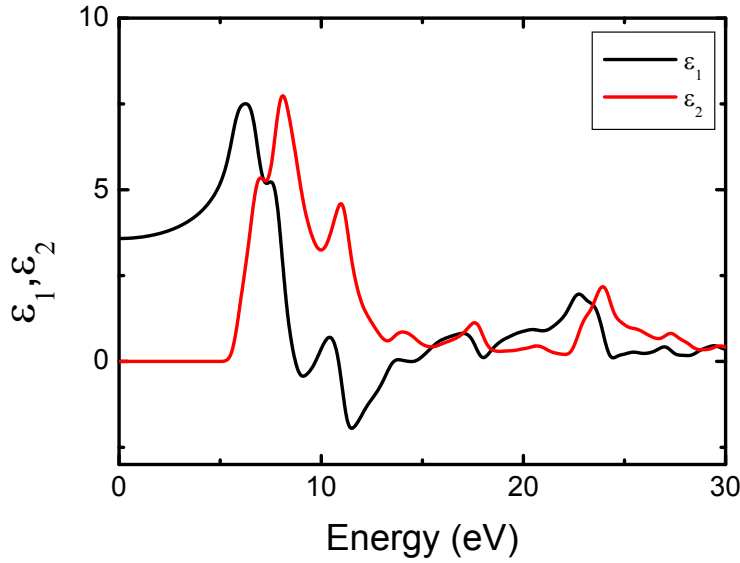


FIG. 5. Real and imaginary parts of dielectric function for c-HfO₂ obtained by GGA+ U^d+U^p .

introducing on-site Coulomb interactions into $5d$ orbital of Hf atom (U^d) and $2p$ orbital of O atom (U^p) at the same time. We obtain the best estimations of U^d and U^p for c-HfO₂. The electron structure and optical properties are calculated both by GGA and GGA + U^d ($U^d = 8.25$ eV) + U^p ($U^p = 6.25$ eV). We find that a shoulder structure below the main peak of the imaginary part of the dielectric constant remains even when U^d and U^p are introduced. This implies that the shoulder structure is robust, and we thus expect that the shoulder appears in the optical measurements for pure c-HfO₂ samples. These findings imply that the GGA+ U^d+U^p approach is a powerful method to calculate and predict the electronic structures and optical properties of wide-gap optical materials.

ACKNOWLEDGMENTS

The authors thank Prof. Vladimir I. Anisimov and Dr. Alexey Shorikov, Institute of Metal Physics, Russian Academy of Sciences, for their valuable discussions.

REFERENCES

- ¹B. E. Weir, P. J. Silverman, M. Alam, F. Baumann, D. Monroe, A. Ghetti, D. Bude, G. L. Timp, A. Hamad, T. M. Oberdick, N. X.

- Zhao, Y. Ma, M. M. Brown, D. Hwang, T. W. Sorsch, and J. Madic, in *Electron Devices Meeting, 1999. IEDM '99. Technical Digest. International* (1999) pp. 437–440.
- ²M. Cao, P. Vande Voorde, M. Cox, and W. Greene, *IEEE Electron Device Lett.* **19**, 291 (1998).
- ³G. He, L. Zhu, M. Liu, Q. Fang, and L. Zhang, *Appl. Surf. Sci.* **253**, 3413 (2007).
- ⁴M. Gilo and N. Croitoru, *Thin Solid Films* **350**, 203 (1999).
- ⁵K. Yamamoto, S. Hayashi, M. Kubota, and M. Niwa, *Appl. Phys. Lett.* **81**, 2053 (2002).
- ⁶R. Terki, G. Bertrand, H. Aourag, and C. Coddet, *Mater. Lett.* **62**, 1484 (2008).
- ⁷T. A. Lee and A. Navrotsky, *J. Mater. Res.* **19**, 1855 (2004).
- ⁸L. Shi, Y. Zhou, J. Yin, and Z. Liu, *J. Appl. Phys.* **107**, 014104 (2010).
- ⁹X. Zhao and D. Vanderbilt, *Phys. Rev. B* **65**, 233106 (2002).
- ¹⁰G.-M. Rignanese, X. Gonze, G. Jun, K. Cho, and A. Pasquarello, *Phys. Rev. B* **69**, 184301 (2004).
- ¹¹R. Terki, H. Feraoun, G. Bertrand, and H. Aourag, *Comp. Mater. Sci.* **33**, 44 (2005).
- ¹²J. C. Garcia, A. T. Lino, L. M. R. Scolfaro, J. R. Leite, V. N. Freire, G. A. Farias, and J. E. F. da Silva, *AIP Conf. Proc.* **772**, 189 (2005).
- ¹³H. Jiang, R. I. Gomez-Abal, P. Rinke, and M. Scheffler, *Phys. Rev. B* **81**, 085119 (2010).
- ¹⁴V. I. Anisimov, F. Aryasetiawan, and A. I. Lichtenstein, *J. Phys.: Condens. Matter* **9**, 767 (1997).
- ¹⁵H. Jiang, R. I. Gomez-Abal, P. Rinke, and M. Scheffler, *Phys. Rev. B* **82**, 045108 (2010).
- ¹⁶J. J. Plata, A. M. Márquez, and J. F. Sanz, *J. Chem. Phys.* **136**, 041101 (2012).
- ¹⁷C. Loschen, J. Carrasco, K. M. Neyman, and F. Illas, *Phys. Rev. B* **75**, 035115 (2007).
- ¹⁸M. D. Segall, P. J. D. Lindan, M. J. Probert, C. J. Pickard, P. J. Hasnip, S. J. Clark, and M. C. Payne, *J. Phys.: Condens. Matter* **14**, 2717 (2002).
- ¹⁹Q. Liu, Z. Liu, L. Feng, and B. Xu, *Physica B: Condens. Matter* **404**, 3614 (2009).
- ²⁰J. Wang, H. Li, and R. Stevens, *J. Mater. Sci.* **27**, 5397 (1992).
- ²¹J.-W. Park, D.-K. Lee, D. Lim, H. Lee, and S.-H. Choi, *J. Appl. Phys.* **104**, 033521 (2008).
- ²²S.-G. Lim, S. Kriventsov, T. N. Jackson, J. H. Haeni, D. G. Schlom, A. M. Balbashov, R. Uecker, P. Reiche, J. L. Freeouf, and G. Lucovsky, *J. Appl. Phys.* **91**, 4500 (2002).

²³M. Koike, T. Ino, Y. Kamimuta, M. Koyama, Y. Kamata, M. Suzuki, Y. Mitani, and A. Nishiyama, Phys. Rev. B **73**, 125123 (2006).